Marine Chemistry 173 (2015) 183–194

Contents lists available at ScienceDirect

Marine Chemistry

journal homepage: www.elsevier.com/locate/marchem

Iron-binding ligands and humic substances in the San Francisco Bay estuary and estuarine-influenced shelf regions of coastal California

Randelle M. Bundy [a,*], Hussain A.N. Abdulla [b], Patrick G. Hatcher [b], Dondra V. Biller [c], Kristen N. Buck [d], Katherine A. Barbeau [a]

[a] Scripps Institution of Oceanography, University of California San Diego Geosciences Research Division, 9500 Gilman Drive, La Jolla, CA, 92093, USA
[b] Department of Ocean, Earth, and Atmospheric Sciences, Old Dominion University, 5115 Hampton Blvd., Norfolk, VA, 23529, USA
[c] University of California Santa Cruz, Department of Ocean Sciences, 1156 High St., Santa Cruz, CA, 95064, USA
[d] University of South Florida, College of Marine Science, 140 7th Ave., St. Petersburg, FL, 33701, USA

ARTICLE INFO

Article history:
Received 24 May 2014
Received in revised form 29 October 2014
Accepted 4 November 2014
Available online 20 November 2014

Keywords:
Estuaries
Organic matter
Flocculation
Iron
Iron-binding ligands
Humic substances
Aliphatic polycarboxylic compounds
Proton nuclear magnetic resonance
Cathodic stripping voltammetry
Multiple analytical window
USA, California, San Francisco Bay

ABSTRACT

Dissolved iron (dFe) and organic dFe-binding ligands were determined in San Francisco Bay, California by competitive ligand exchange adsorptive cathodic stripping voltammetry (CLE-ACSV) along a salinity gradient from the freshwater endmember of the Sacramento River (salinity <2) to the mouth of the estuary (salinity >26). A range of dFe-binding ligand classes was simultaneously determined using multiple analytical window analysis, involving titrations with multiple concentrations of the added ligand, salicylaldoxime. The highest dFe and ligand concentrations were determined in the low salinity end of the estuary, with dFe equal to 131.5 nmol L^{-1} and strong ligand ($\log K^{cond}_{FeL,Fe'} \geq 12.0$) concentrations equal to 139.5 nmol L^{-1}. The weakest ligands ($\log K^{cond}_{FeL,Fe'} < 10.0$) were always in excess of dFe in low salinity waters, but were rapidly flocculated within the estuary and were not detected at salinities greater than 7. The strongest ligands ($\log K^{cond}_{FeL,Fe'} > 11.0$) were tightly coupled to dFe throughout the estuary, with average excess ligand concentrations ([L]–[dFe]) equal to 0.5 nmol L^{-1}. Humic-like substances analyzed via both CLE-ACSV and proton nuclear magnetic resonance in several samples were found to be a significant portion of the dFe-binding ligand pool in San Francisco Bay, with concentrations ranging from 559.5 μg L^{-1} to 67.5 μg L^{-1} in the lowest and highest salinity samples, respectively. DFe-binding ligands and humic-like substances were also found in benthic boundary layer samples taken from the shelf near the mouths of San Francisco Bay and Eel River, suggesting estuaries are an important source of dFe-binding ligands to California coastal shelf waters.

© 2014 Elsevier B.V. All rights reserved.

1. Introduction

Iron (Fe) is a growth-limiting micronutrient for phytoplankton in many regions of the oceans, including even some coastal upwelling regions (Biller and Bruland, 2014; Bruland et al., 2001, 2005; King and Barbeau, 2007). This is especially true in the California Current System (CCS), a highly productive coastal region dominated by diatom growth during the spring upwelling season (Bruland et al., 2001; Hutchins et al., 1998). Although dissolved Fe (dFe) is widely recognized as a limiting nutrient, less is understood about its chemical speciation in seawater, which affects its reactivity and availability to the biological community. It is known that dFe-binding ligands are essential for maintaining dFe in solution above its thermodynamic inorganic solubility limit (Liu and Millero, 2002) and they bind the majority of the dFe in seawater (Gledhill and van den Berg, 1994; Rue and Bruland, 1995; van den berg, 1995). Organic compounds that bind dFe appear to be ubiquitous and are likely a heterogeneous mixture of complexes (Gledhill and Buck, 2012). The types of dFe-binding organic ligands present in seawater are thought to range from relatively weak macromolecules and cellular byproducts such as polysaccharides (Hassler

Abbreviations: $\alpha_{Fe(SA)_x}$, the side reaction coefficient for the iron-salicylaldoxime complex; BBL, benthic boundary layer; CCS, California Current System; CLE-ACSV, competitive ligand exchange adsorptive cathodic stripping voltammetry; CO_2, carbon dioxide; COSY, correlation spectroscopy; CRAM, carboxylic rich alicyclic molecules; CSV, cathodic stripping voltammetry; CTD, conductivity, temperature, and depth sensor; dFe, dissolved Fe; DOC, dissolved organic carbon; tDOC, terrestrial dissolved organic carbon; DOM, dissolved organic matter; Fe, iron; FPE, fluorinated polyethylene; FTIR, Fourier transform infrared spectroscopy; HSAB, hard and soft acids and bases; HMW, high molecular weight; ^{1}H-NMR, proton nuclear magnetic resonance; HPS, heteropolysaccharides; HS, humic-like substances; HSQC, heteronuclear single quantum coherence; ICP-MS, inductively coupled plasma mass spectrometry; KHP, potassium hydrogen phthalate; LDPE, low density polyethylene; L_x, an iron binding ligand class, where *x* denotes ligand class (1–4); $\log \alpha_{L_T}$, combined side reaction coefficient of all ligands detected; $\log K^{cond}_{FeL,Fe'}$, the conditional stability constant of iron-binding ligands; MAW, multiple analytical window analysis; Milli-Q, purified water; POM, particulate organic matter; Pt, platinum; *S*, salinity; SA, salicylaldoxime; SAFe, sampling and analysis of iron (Fe); USGS, United States Geological Survey.

* Corresponding author at: Scripps Institution of Oceanography/University of California, San Diego, 9500 Gilman Drive MC 0208, La Jolla, CA, 92093, USA. Tel.: +1 858 534 1532.
E-mail address: rmbundy@ucsd.edu (R.M. Bundy).

http://dx.doi.org/10.1016/j.marchem.2014.11.005
0304-4203/© 2014 Elsevier B.V. All rights reserved.

et al., 2011a) and humics (Laglera and van den Berg, 2009), to low-molecular weight siderophore-like complexes such as hydroxamates (Mawji et al., 2011; Velasquez et al., 2011), and catecholates (Poorvin et al., 2011). Although only hydroxamates have thus far been directly isolated from seawater, indirect methods for detecting metal-binding ligands such as competitive ligand exchange-adsorptive cathodic stripping voltammetry (CLE-ACSV) can provide important insight on the characteristics of the ligand pool in seawater (see review by Gledhill and Buck, 2012).

Identifying the sources of dFe-binding ligands in seawater is an active area of research, and ligands are important in the mechanism of dFe delivery to many marine ecosystems. One such ecosystem may be the CCS, where the majority of the dFe supply is hypothesized to come from Fe-rich sediment sources along the continental shelf, ranging in character from narrow rocky shelves with low dFe to wide-shelf mudflats with high dFe near San Francisco Bay and Eel River (Biller et al., 2013; Elrod et al., 2004). High dFe concentrations have been observed in surface waters over the wide region of the shelf in the spring during the onset of upwelling (Biller et al., 2013; Elrod et al., 2008). Concentrations of dFe have been reported to increase during the initial upwelling period and decrease slowly thereafter, despite continued intensification of the upwelling (Elrod et al., 2008). This has led to the suggestion that the wide shelf regions act as "capacitors" for dFe, charging with riverine-derived Fe during the winter flood season and discharging Fe when the Fe-rich sediments are resuspended during the initial spring upwelling phase (Bruland et al., 2001; Chase et al., 2007). Mudflats in the wide shelf region may also be a source of organic ligands, and high concentrations of strong dFe-binding ligands have been observed in the benthic boundary layer (BBL) in this region (Buck et al., 2007; Bundy et al., 2014). If these organic ligands, like the dFe with which they are associated, are primarily from terrestrial sources, then we would expect that the organic Fe-complexes in the BBL should be similar to those in local freshwater and estuarine sources such as San Francisco Bay. Previous studies have examined the binding strengths of dFe–ligand complexes in the high salinity end of the San Francisco Bay plume (Buck et al., 2007; Bundy et al., 2014), but there have been no studies of dFe-binding ligands in lower salinity waters in the San Francisco Bay estuary.

In early classic work on Fe across salinity gradients in estuarine systems, Boyle et al. (1977) found that up to 90% of the dFe in estuaries is lost to scavenging, mostly due to flocculation of humic-like substances (HS) and dFe at low salinities. Sholkovitz et al. (1978) expanded these observations to add that most of the lost dFe occurred in the colloidal size fraction. The chemical form of the small amount of dFe that survives flocculation is still unclear, however, and it is possible that organic complexation of dFe by HS plays a role in stabilizing dFe concentrations across salinity gradients. Some studies have examined the role of HS in dFe speciation in estuarine and coastal environments, using combined information about dFe binding strengths and HS distributions in the Irish Sea (Laglera and van den Berg, 2009) and Thurso Bay (Batchelli et al., 2010). Characterization of the HS pool in some studies has also shown that the high concentration of oxygen-containing functional groups in terrestrial HS is largely responsible for terrestrial dissolved organic matter (tDOM) reactivity (Stevenson, 1994), and of these functional groups, carboxyl groups are the most abundant (Cabaniss, 1991; Hatcher et al., 1981; Leenheer et al., 1995; Stevenson, 1994) and have the ability to complex dFe. In this study we examined multiple classes of dFe-binding ligands and HS using CLE-ACSV, in samples collected along a salinity gradient in San Francisco Bay. Two BBL samples were also examined, from the adjacent continental shelf in the San Francisco Bay region and from the Eel River shelf system further north. In several samples we applied proton nuclear magnetic resonance (^{1}H-NMR) to complement our CLE-ACSV analysis and provide insight into the possible chemical character of organic Fe binding groups.

This work follows on a recently published study of dFe-binding ligands in the CCS (Bundy et al., 2014), in which a multiple analytical window (MAW) CLE-ACSV approach was applied to dFe-binding ligands in order to detect several ligand classes. The method used by Bundy et al. (2014) enabled the simultaneous detection of a wide range of dFe-binding ligands (L_1–L_4), each with distinct distributions in the CCS. The authors hypothesized these ligand classes to be composed of siderophore-like ligands (L_1, $\log K^{cond}_{FeL_1,Fe'} \geq 12.0$), HS ($L_2$, $\log K^{cond}_{FeL_2,Fe'}$ 11–12), degradation products of the stronger ligand classes (L_3, $\log K^{cond}_{FeL_3,Fe'}$ 10–11) and relatively weak macromolecules with incidental Fe binding (L_4, $\log K^{cond}_{FeL_4,Fe'} < 10$). HS was also measured directly by Bundy et al. (2014) using cathodic stripping voltammetry (CSV) (Laglera et al., 2007), which confirmed the presence of HS-like material in the BBL of mudflat regions of the California continental shelf (Bundy et al., 2014). The source of these compounds is unknown, but is thought to originate from estuarine regions such as San Francisco Bay. It is apparent from recent work (Batchelli et al., 2010; Bundy et al., 2014; Laglera and van den Berg, 2009) that some portion of terrestrial-derived HS material is resistant to flocculation in coastal estuaries, but how much is delivered to the shelf in the CCS region is an open question. This study seeks to identify the source of dFe-binding ligand complexes to the broad, estuarine-influenced shelf areas of coastal California, and characterize changes in the dFe ligand pool across an estuarine salinity gradient by employing MAW CLE-ACSV, in combination with ^{1}H-NMR and HS analysis for some samples.

2. Methods

2.1. Sampling

Samples were collected in partnership with the United States Geological Survey (USGS) on board the R/V Polaris on April 19, 2011 as part of the regular USGS San Francisco Bay Water Quality Measurement Program (http://sfbay.wr.usgs.gov/access/wqdata/index.html). Hydrographic data was collected for all 24 regular stations in the

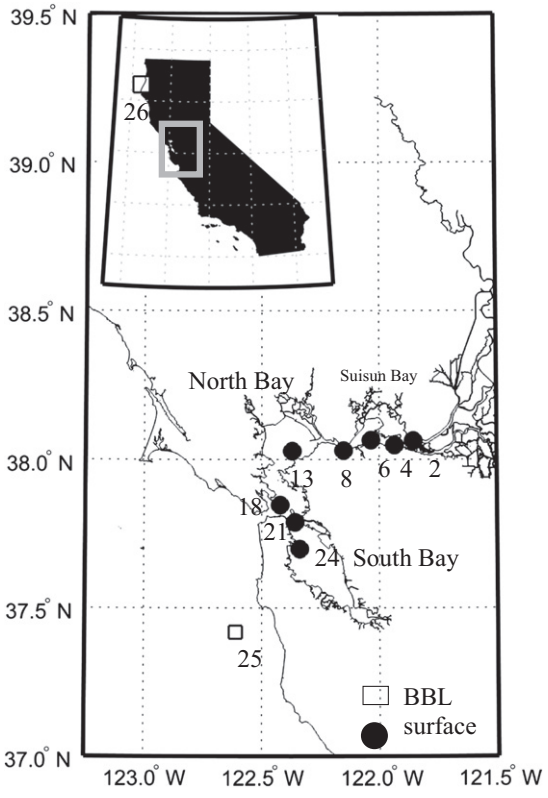

Fig. 1. Dissolved Fe (dFe) and dFe-binding ligand surface sampling locations in San Francisco Bay (filled circles; stations 2, 4, 6, 8, 13, 18, 21, and 24) and the California continental shelf benthic boundary layer (BBL, open squares; stations 25 and 26).

North Bay and Central Bay, and a subset of eight stations were sampled for dFe, organic dFe-binding ligands, and humic-like substance (HS) analyses (Fig. 1). Hydrographic data in San Francisco Bay was obtained using a conductivity, temperature and depth (CTD) sensor outfitted with an oxygen electrode (Sea-bird Electronics), optical backscatter sensor (D&A Instruments), and a fluorometer (Turner Designs). Discrete samples were also taken for nitrate measurements (nitrate + nitrite) and other inorganic nutrients and analyzed by colorimetric methods (http://sfbay.wr.usgs.gov/access/wqdata/overview/measure/index.html). Two additional samples were also obtained for HS analyses (see Section 2.4) from a previous cruise (Bundy et al., 2014) in the benthic boundary layer (BBL, stations 25 and 26) outside of San Francisco Bay and Eel River, the two main freshwater influences on the CCS. Details about the hydrographic and ligand data of the BBL samples collected in August/September 2011 on board the R/V Point Sur (see Biller et al., 2013) can be found in Bundy et al. (2014).

DFe and dFe-binding ligand samples were collected using trace metal clean Teflon tubing and a Teflon diaphragm pump (Cole Parmer) connected to an air compressor. A small Teflon coated weight was fixed to the end of the pump tubing, and the tubing was lowered approximately 2 m below the surface off the starboard side of the ship. A fiberglass pole was used to extend tubing approximately 2 m away from the starboard side and samples were collected while the ship was moving forward at approximately 1 knot. Samples were filtered in-line with an acid-cleaned 0.45 μm Osmonics cartridge filters (GE Osmonics) after 1 L of water had been passed through the tubing and filter. DFe samples were stored at room temperature in 250 mL acid-cleaned low density polyethylene (LDPE) bottles (Nalgene) at pH 1.8 (Optima HCl, Fisher Scientific). DFe-binding ligand and HS samples were placed in two 500 mL fluorinated polyethylene (FPE) bottles (Nalgene) and immediately frozen (-20 °C) until analysis.

2.2. Dissolved iron

DFe samples were analyzed according to Biller and Bruland (2012), building on earlier work of Sohrin et al (2008). This multi-elemental analysis method utilizes an offline pre-concentration step after pH adjustment (pH = 6.2) of acidified samples onto the Nobias-chelate PA1 resin (Hitachi High-Technologies; Sohrin et al., 2008). After pre-concentration in a closed-column manifold, the columns are rinsed with ammonium acetate and the trace metals are subsequently eluted using 1 N quartz distilled nitric acid (Fisher Scientific). Samples were measured using magnetic sector inductively coupled plasma mass spectrometry (ICP-MS). For dFe, the recovery from the column was greater than 98%, with an average blank equal to 0.030 nmol kg^{-1} and a detection limit of 0.014 nmol kg^{-1}. This method had excellent agreement with reported consensus values for SAFe (Johnson et al., 2007) and GEOTRACES reference samples (www.geotraces.org), yielding values for S1 of 0.091 ± 0.001 nmol kg^{-1} (0.093 ± 0.008 nmol kg^{-1} consensus value as of May 2013) and 0.98 ± 0.009 nmol kg^{-1} for D2 (0.933 ± 0.023 nmol kg^{-1} consensus value).

2.3. Dissolved iron-binding ligands

Organic dFe-binding ligands were analyzed using a multiple analytical window (MAW) adaptation (Bundy et al., 2014) of traditional competitive ligand exchange-adsorptive cathodic stripping voltammetry (CLE-ACSV) methods (see Buck et al., 2012 for an intercomparison of these methods). Competitive ligand approaches utilize a well-characterized added ligand to set up a competition between the added ligand and the natural ligands present in the sample. The added ligand, in this case salicylaldoxime (SA), makes an electro-active complex with the dFe in the sample and the $Fe(SA)_x$ complex adsorbs to the mercury drop of a controlled growth mercury electrode (CGME, Bioanalytical Systems Incorporated). The dFe is then reduced and stripped from the $Fe(SA)_x$ complex (cathodic stripping) and the change in current is recorded by the analyzer (Epsilon 2, Bioanalytical Systems Incorporated) connected to a laptop computer. The peak height at each titration point can then be related to the amount of $Fe(SA)_x$ formed, and the remaining speciation can be calculated via the sensitivity and mass balance.

2.3.1. Ligand titrations

In order to set-up each titration, individual acid-cleaned Teflon vials were first conditioned to the expected dFe addition for 24 hours. Then, 10 mL aliquots of the sample were placed in 10 different vials along with 50 μl of a 1.5 M boric acid buffer (pH 8.2, NBS scale) made in 0.4 mol L^{-1} ammonium hydroxide (Optima, Fisher Scientific). The buffer and added dFe (0–100 nmol L^{-1}) were left to equilibrate for at least 2 hours. The competitive ligand SA was then added to each vial (9–33 μmol L^{-1}) and was equilibrated for 15 minutes. The contents from each vial were placed into a Teflon cell and were analyzed consecutively via ACSV.

2.3.2. Multiple analytical window approach

The MAW approach used by Bundy et al. (2014) involves doing multiple titrations for each sample with a different concentration of the added ligand, yielding different competition strengths of SA. Five analytical windows were employed in this study, ranging in [SA] from 9 to 33 μmol L^{-1}. The highest analytical window (33 μmol L^{-1} SA, window 1) was the same in every sample, and this titration was used as an "overload" titration to determine only the sensitivity in each sample (see Section 2.3.3); no ligand concentrations were determined from these titrations. The other four analytical windows (windows 2–5) were used for determining four separate ligand classes (L_1–L_4). The analytical window is expressed as the side reaction coefficient, $\alpha_{Fe(SA)_x}$, of the added ligand, determined by

$$\alpha_{Fe(SA)_x} = K^{cond}_{Fe(SA)} \times [SA] + \beta^{cond}_{Fe(SA)_2} \times [SA]^2 \quad (1)$$

where $K^{cond}_{Fe(SA)}$ and $\beta^{cond}_{Fe(SA)_2}$ are the conditional stability constants of the mono and bis-SA complex with dFe. The strength of SA has been carefully characterized in previous studies under marine (Abualhaija and van den Berg, 2014) and estuarine (Buck et al., 2007) conditions. All $\alpha_{Fe(SA)_x}$ constants used in this study were determined based on the most recent calibration of SA (Abualhaija and van den Berg, 2014) and corrected for salinity effects on $\alpha_{Fe(SA)_x}$ (Buck et al., 2007). Slightly different concentrations of SA were used in each sample (with the exception of the overload titration) at each analytical window in order to have a similar $\alpha_{Fe(SA)_x}$ in each sample because of the effect of salinity on $\alpha_{Fe(SA)_x}$. Although salinities were determined at each station using the CTD, salinities were also measured in individual speciation samples to account for any differences in salinity due to different collection depths with the trace metal pump and the ship's CTD. The salinity in speciation samples was measured using an aliquot from the speciation bottles and a hand-held digital refractometer. The salinity was found to vary by up to 2 salinity units (psu) between the salinity measured in the field by the CTD vs. the refractometer in the lab, and thus the salinity determined in each bottle was used to calculate the $\alpha_{Fe(SA)_x}$ and these salinity values are also presented with the speciation data.

2.3.3. Determination of the sensitivity

The sensitivity of the method is often determined by internal calibration of the linear portion of the titration curve, where the majority of ligands in the sample have been titrated by added dFe (Rue and Bruland, 1995). However, it has been shown recently that HS may interfere slightly with the sensitivity determination in CLE-ACSV when SA is the added ligand (Laglera et al., 2011). High ligand and surfactant concentrations in estuarine samples also make the determination of the "true" sensitivity difficult in these samples, especially in lower salinity samples where low sensitivities were particularly apparent. "Overload" titrations were therefore employed at the highest analytical window (33 μmol L^{-1} SA) in order to outcompete all ligands in the sample and

ensure an accurate determination of the sensitivity, while still accounting for any surfactant effects in the sample (Bundy et al., 2014; Kogut and Voelker, 2001). This "overload" sensitivity was then corrected by a ratio in order to obtain the sensitivities at lower concentrations of SA (windows 2–5; Hudson et al., 2003). "Overload" sensitivities in each sample are presented in the supplementary information (S-1). A constant R_{AL} was used for each window, corresponding to a value of 0.7, 0.5, 0.4, and 0.2 for windows 2–5, respectively.

2.3.4. Data processing

Ligand concentrations and strengths were determined based on the averages of van den berg/Ružić and Scatchard linearizations at each analytical window (Buck et al., 2012; Mantoura and Riley, 1975; Scatchard, 1949). Several novel data processing methods have been developed however, so data was also fit using a publicly available multiple detection window analytical tool for general comparison (see Section 2.3.5). Only one ligand class was determined at each analytical window, and characterized as L_1–L_4 based on the absolute strength of the ligand according to recommendations from Gledhill and Buck (2012). This study defines L_1 as ligands with log $K^{cond}_{FeL,Fe'} \geq 12.0$, L_2 with $12.0 >$ log $K^{cond}_{FeL,Fe'} \geq 11.0$, L_3 with a log $K^{cond}_{FeL,Fe'}$ range of $11.0 >$ log $K^{cond}_{FeL,Fe'} \geq 10.0$ and L_4 with a log $K^{cond}_{FeL,Fe'} < 10.0$. L_1 ligands were determined at the highest analytical window, just below the "overload" titration window and each subsequent ligand class was determined at progressively lower analytical windows, using the optimal analytical window for that particular ligand class (Bundy et al., 2014). Additionally, the titrations at each subsequent analytical window were designed to titrate the ligand class determined at the higher [SA] within the first few titration points, and the remainder of the titration was aimed at detecting any additional ligand classes. A ligand was "not detected" if the conditional stability constant of a ligand class determined at one analytical window was identical to that at a higher analytical window. For example, if a ligand with a log $K^{cond}_{FeL,Fe'} = 10.0$ was determined at both windows 4 and 5, then that sample would be deemed to contain no L_4 ligands since no ligands were measured with a log $K^{cond}_{FeL,Fe'} < 10.0$.

2.3.5. Data processing comparison

Several methods are in the intercalibration stages for processing multiple analytical window CLE-ACSV data (Giambalvo, 1997; Hudson et al., 2003; Omanović et al., 2015; Pižeta et al., in review; Sander et al., 2011). None of these methods have been tested yet for dFe organic speciation, but two of the methods are currently available for download from the website of Scientific Committee on Oceanic Research (SCOR) working group 139: "Organic Ligands-A key Control on Trace Metal Biogeochemistry in the Ocean" (http://neon.otago.ac.nz/research/scor/links.html). To ensure there was no overlap in our ligand detection and that our ligand parameters could accurately fit the titration data, the data from each detection window was fit using a modification of the Hudson (unpubl.; Pižeta et al., in review) simultaneous multi-window approach adapted for dFe organic speciation, as a proof of concept. This tool is available online (https://sites.google.com/site/kineteql/home/about-kineteql) and incorporates a KINETEQL equilibrium solver add-in for Microsoft Excel (Giambalvo, 1997) to the approach developed by Hudson et al. (2003) and Sander et al. (2011). This method for titration interpretation will be further referred to as the "Hudson" protocol throughout the article. This method only allows for the detection of three ligand classes, so a comparison was made between the L_3 determined by the Hudson multi-window tool and $L_3 + L_4$ found in this study (SI-3).

2.4. Humic-like substance analysis by CSV

Humic-like substances (HS) were measured in five San Francisco Bay samples (stations 2, 13, 24, 25 and 26) in order to assess the potential contribution of HS to the dFe-binding ligand pool. The [HS] at stations 25 and 26 were presented previously in Bundy et al. (2014), and this study expands those measurements to include proton nuclear magnetic resonance (^{1}H-NMR) data. Four of the five stations where HS was measured by CSV were analyzed using ^{1}H-NMR (stations 13, 24, 25 and 26), as described in Section 2.6. HS by CSV were measured according to the methods described in Laglera et al. (2007). Briefly, a 20 mg L^{-1} stock solution of Suwannee River Fulvic Acid Standard (International Humic Substance Society) was prepared in purified water (Milli-Q water, 18 mol L^{-1} Ω cm) and added to 10 mL sample aliquots along with boric acid-ammonia buffer (pH 8.2, NBS scale) and dFe (100 nmol L^{-1}, secondary stock solutions made from an AA standard). Three vials contained no added HS, while the rest of the vials contained 5–150 μg L^{-1} HS and were left to equilibrate for at least 2 hours. Immediately before analysis by CSV, 400 μl of 0.4 mol L^{-1} potassium bromate was added in order to catalyze the reaction without oxidizing the HS. Each aliquot was analyzed separately using CSV as described by Laglera et al. (2007) using the standard addition method. This method measures all organic substances that bind dFe and are shown to be "humic-like," or contributing to the electrochemical peak at −0.6 V.

2.5. Dissolved organic carbon (DOC)

Samples for dissolved organic carbon (DOC) were taken from stations 13, 24, 25 and 26 and run in triplicate. Aliquots from the speciation bottles were taken and placed in 60 mL glass bottles and acidified to pH 2 with 6 M phosphoric acid before analysis. DOC concentrations were measured on a Shimadzu TOC-V Combustion Analyzer using high temperature (680 °C) platinum (Pt)-catalyzed oxidation coupled to non-dispersive infrared gas detection of carbon dioxide (CO_2). Calibration standards were prepared using a potassium hydrogen phthalate (KHP) standard.

2.6. Proton nuclear magnetic resonance (^{1}H-NMR) analysis

The dissolved organic matter (DOM) from four stations (13, 24, 25, and 26) was characterized by ^{1}H-NMR at its natural DOM concentration without prior pretreatment. All the ^{1}H-NMR experiments were acquired using a Bruker Avance III 400 spectrometer. D_2O (>99.9%, Aldrich Chemical Company, Milwaukee, WI) was added to 0.5 mL of the sample at a ratio of 10:90 in 5-mm glass NMR tubes (Wilmad Glass Co., NJ). Solution state ^{1}H-NMR spectra were acquired using a water suppression technique originally described by Lam and Simpson (2008) with modification. A recycle delay of 2 s was used along with a 119 ms acquisition time. Using the water suppression techniques slightly attenuates the carbohydrate signal around 3.5 ppm (Lam and Simpson, 2008); however, by using this technique we insured a complete suppression of the water peak. The ^{1}H-NMR spectra were then normalized to their total area (0.20–10.00 ppm) and vertically scaled by a factor of 1000. Using this technique allows for characterization the entire DOM pool without any fractionation, isolation or sample pre-treatment.

3. Results

3.1. Hydrographic data

All hydrographic data was collected by the USGS San Francisco Bay Water Quality Measuring Program and can be found in their database (http://sfbay.wr.usgs.gov/access/wqdata/index.html). The stations sampled ranged from the freshwater endmember of the Sacramento River (salinity, S; < 2), past the mouth of San Francisco Bay (S; > 21), and into the northern third of South Bay ($18 < S < 21$; Figs. 1 and 2). The maximum salinity was measured in Central Bay at station 18, with lower salinities in South Bay (station 24) and closer to the Sacramento River (station 2). The temperature ranged from 13 to 15 °C, with higher temperatures in the low salinity region of North Bay (Fig. 2). Nitrate (nitrite + nitrate) ranged from 7.6 μmol L^{-1} at station

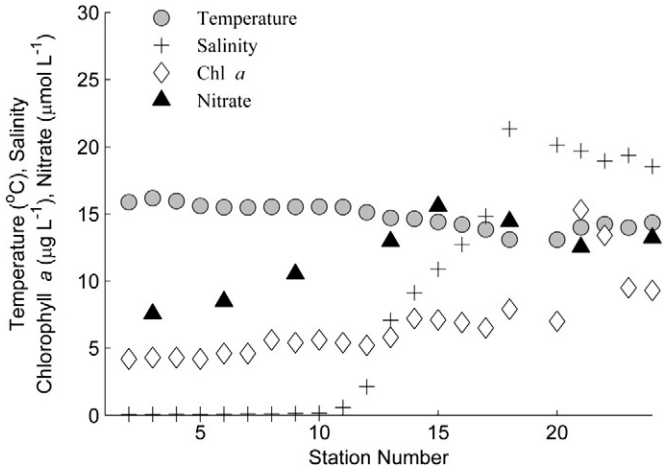

Fig. 2. Temperature (°C), salinity, nitrate + nitrite (μmol L^{-1}) and chlorophyll *a* (μg L^{-1}) concentrations at each USGS sampling location in San Francisco Bay.

3 to a maximum of 15.6 μmol L^{-1} at station 15 in Central Bay. Elevated chlorophyll *a* concentrations were observed at stations 21 and 22 in the upper region of South Bay (15.3 and 13.4 μg L^{-1}, respectively; Fig. 2).

3.2. Dissolved iron

DFe concentrations were highest in the low salinity end of the bay, and decreased towards the mouth of San Francisco Bay (Fig. 3A), as observed in many other estuarine studies (e.g. Boyle et al., 1977; Buck et al., 2007; Murray and Gill, 1978; Sholkovitz et al., 1978). The non-conservative behavior in [dFe] with increasing salinities indicates either (1) there is a net sink of dFe due to flocculation; (2) the time scale of variation in [dFe] for the marine and freshwater endmembers is shorter than the flushing time of San Francisco Bay; or (3) there is mixing from multiple freshwater endmembers that have different [dFe]. The highest [dFe] was measured at station 8 in Suisun Bay (Fig. 1), and was 131.5 nmol L^{-1}. This likely reflects the additional freshwater [dFe] and ligand sources from the Suisun Slough. The lowest [dFe] in San Francisco Bay was 7.0 nmol L^{-1}at station 21 in Central Bay. The highest [dFe] were found at the lower salinities in general, although the lowest salinity sample (station 2) did not have the highest [dFe] (station 8) and higher variability was seen in low salinity samples (Fig. 3A).

3.3. Ligand data comparison

The dFe-binding ligand results from this study were compared between two different interpretation approaches: the conventional discrete linearizations approach and the unified Hudson protocol (Giambalvo, 1997; Hudson et al., 2003; Sander et al., 2011), modified for dFe organic speciation. Although the Hudson method has not been tested yet for dFe speciation, a unified approach to analyzing multiple analytical window data sets has been shown for copper speciation to yield better results than interpreting single window data alone (Pižeta et al., in review; Sander et al., 2011). Updated constants for SA were used for the interpretations, and R_{AL} was set to the values calculated in this work (1.0, 0.7, 0.5, 0.4, 0.2; SI-2). The initial guess for the sensitivity and ligand parameters in the Hudson protocol were set to the overload sensitivity determined in that sample and the ligand concentrations determined by the linearization techniques for this work. Since only three ligands can be currently calculated in the Hudson protocol regardless of number of analytical windows employed, we compared [L_3] from the Hudson method to [L_3 + L_4] from the linearization output. A comparison of the results between both approaches is shown in SI-3, with good agreement seen between the two methods ($r^2 = 0.87$), particularly with the ligand concentrations. Poorer agreement was seen with the log $K^{cond}_{FeL,Fe'}$, where the log *K* was systematically higher in the Hudson protocol results (SI-3). Overall, the good agreement between methods ensured we were not getting overlapping ligand concentrations in our different analytical windows, and that linearization techniques compare relatively well with unified analytical window data processing approaches currently under development.

3.4. Dissolved iron organic speciation

DFe-binding organic ligands are expressed as operationally defined ligand classes, distinguished simply by their conditional stability constants (Bundy et al., 2014). Traditionally, in the literature "L_1" and "L_2" ligands are determined based on their relative strengths, while the classification in this paper is based on absolute strengths. Multiple analytical window (MAW) analysis enables the detection a much broader range of ligand strengths than have been observed in the literature by any one study (Gledhill and Buck, 2012). However, in general, the stronger ligands (L_1 and L_2 in this study) are comparable to ligand classes denoted as "L_1" in the literature, and weaker ligands (L_3 and L_4) are comparable to "L_2" in the literature (Bundy et al., 2014; Gledhill and Buck, 2012).

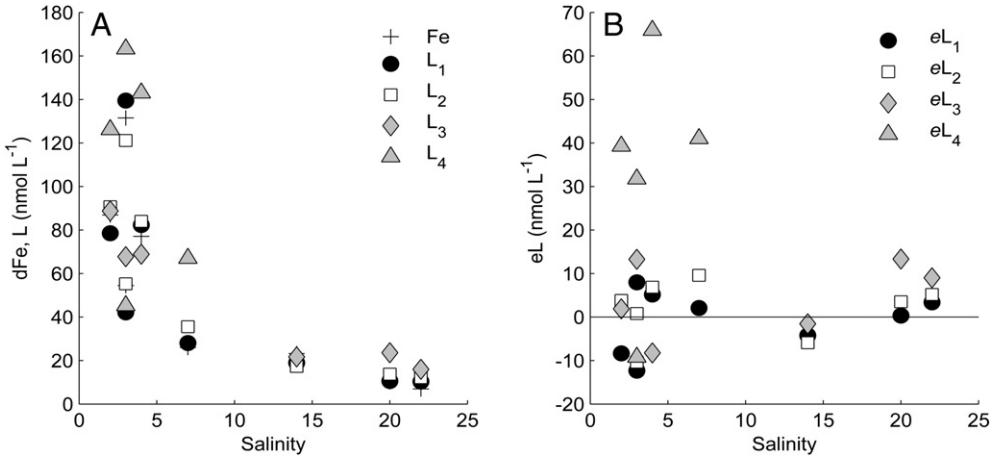

Fig. 3. (A) Dissolved Fe (nmol L^{-1}), and Fe-binding ligand concentrations (L_1, L_2, L_3 and L_4, nmol L^{-1}) in San Francisco Bay. (B) Excess ligand (eL) concentrations ([L_x]–[Fe], nmol L^{-1} where "*x*" denotes ligand class, 1–4), at each station versus salinity.

Table 1
Hydrographic and ligand data for all stations sampled in San Francisco Bay (SF Bay) and in the California Current Ecosystem (CCE). Longitude (Lon., °W), latitude (Lat., °N), sampling depth (Depth, m), temperature (Temp., °C), and chlorophyll *a* concentrations (Chl *a*, μg L^{-1}) were obtained from the USGS San Francisco Bay Water Quality Measuring program (http://sfbay.wr.usgs.gov/access/wqdata/index.html). Salinity (*S*) measurements were taken from individual dFe-binding ligand samples. Ligand classes (L_1–L_4) represent dFe-binding ligands characterized by their log $K^{cond}_{FeL_i,Fe'}$ (log K_1 to log K_4) as described in Section 2.3.4. The concentration of humic substances (HS, μg L^{-1}) was determined according to Laglera et al. (2007) described in Section 2.4. The notation "nd" means not detected, and (*) indicates ligand data that was previously published in Bundy et al. (2014).

Region	Sta.	Lon. (°W)	Lat. (°N)	Depth (m)	Temp. (°C)	*S* (psu)	Chl *a* (μg L^{-1})	dFe (nmol L^{-1})	L_1 (nmol L^{-1})	logK_1	L_2 (nmol L^{-1})	logK_2	L_3 (nmol L^{-1})	logK_3	L_4 (nmol L^{-1})	logK_4	HS (μg L^{-1})
SF Bay	2	121.855	38.063	2.0	15.9	4.2	4.2	77.1	82.3	12.9	84.0	11.7	68.9	10.3	143.0	9.9	559.5
SF Bay	4	121.935	38.048	2.0	16.0	2.3	4.3	86.9	78.5	12.4	90.7	11.7	88.8	10.9	126.2	9.2	nd
SF Bay	6	122.035	38.065	2.0	15.5	3.0	4.6	54.5	42.2	12.8	55.3	11.3	67.7	10.8	45.3	9.6	nd
SF Bay	8	122.152	38.030	2.0	15.5	3.1	5.6	131.5	139.5	12.5	121.2	12.0	nd	nd	163.3	9.2	nd
SF Bay	13	122.370	38.028	2.0	14.7	7.2	5.8	26.0	28.1	13.1	35.6	11.3	nd	nd	67.0	9.9	111.2
SF Bay	18	122.422	37.847	2.0	13.1	14.4	7.9	23.2	19.0	12.3	17.3	11.4	21.7	10.4	nd	nd	nd
SF Bay	21	122.358	37.788	2.0	14.0	22.3	15.3	7.0	10.3	12.2	12.1	11.4	16.0	11.0	nd	nd	nd
SF Bay	24	122.338	37.698	2.0	14.4	20.0	9.3	10.3	10.6	13.2	13.8	11.8	23.6	10.4	nd	nd	67.5
CCE	25*	122.611	37.418	64.0	10.0	33.9	nd	6.8	9.2	12.2	11.3	11.5	nd	nd	nd	nd	39.2
CCE	26*	124.386	40.767	64.0	8.6	33.9	nd	20.5	nd	nd	16.9	11.0	nd	nd	nd	nd	22.6

The strongest ligands were inversely related to salinity in San Francisco Bay (Fig. 3A). The highest [L_1] were found at station 8, where [dFe] was also the highest (Table 1). In order to examine patterns in the ligands that might be de-coupled from the [dFe], "excess" ligand concentrations are also shown in Fig. 3B. "Excess" ligand is defined in this study simply as [L_x]–[dFe], where *x* denotes the ligand class. Excess L_1 ligand concentrations (eL_1; [L_1]–[dFe]) ranged from −12.3 to 7.9 nmol L^{-1} (Fig. 3B), and were relatively tightly coupled to [dFe] compared to the other ligand classes. L_2 ligands showed a similar pattern to L_1, though with higher concentrations and a slightly larger range in [eL_2] (−10.4 to 9.6 nmol L^{-1}).

The weaker ligands (L_3 and L_4) showed a similar pattern with increasing salinity as the stronger ligands and dFe, but with subtle differences (Fig. 3). The highest concentration of L_3 ligands was at station 4, and the lowest at station 21 with 88.8 ± 9.4 nmol L^{-1} and 16.0 ± 0.03 nmol L^{-1}, respectively. Although every station contained detectable stronger ligands, station 8 and 13 did not have detectable L_3 ligands (Table 1) though they were detectable again at higher salinities. The range of [eL_3] was also wider than for the stronger ligands, with a range of −8.2 to 13.3 nmol L^{-1} (Fig. 3B).

L_4 ligands were the most distinct in terms of the patterns within the estuary, and showed de-coupling from the [dFe] (Fig. 3). [L_4] were extremely high within the low salinity end of the estuary (163.3 ± 3.7 nmol L^{-1} at station 8) and were no longer detectable in any samples with salinities above 7. In the stations where L_4 ligands were detected, they were always in excess of the [dFe], leading to large excess ligand concentrations (up to 65.9 nmol L^{-1}). Low salinity samples also had a higher overall complexation capacity (log α_{L_T}; data not shown) based on the potential of contribution of all ligand classes to bind dFe, suggesting the weaker ligands may also effectively compete with stronger ligands for dFe in low salinity waters.

3.5. Humic-like substances

Humic-like substances (HS) were determined by CSV (Laglera et al., 2007) and also inferred from ^{1}H-NMR (Abdulla et al., 2013) in samples in San Francisco Bay and California coastal waters (Fig. 1). HS determined by CSV were found to range from 67.5 μg L^{-1} to 559.5 μg L^{-1} in San Francisco Bay, with the highest concentrations found at station 2, and lower concentrations found at station 24 (Table 1). In general, HS behaved non-conservatively in the estuary like dFe and ligands (Fig. 4). HS were measured by CSV in the two California shelf BBL samples (Bundy et al., 2014), and are also shown in Table 1 for comparison. HS were determined to be part of the L_2 ligand pool in previous work (Bundy et al., 2014) based on the log $K^{cond}_{FeL,Fe'}$ determined by Laglera et al. (2007), which was found to be equal to 11.1–11.6 (Abualhaija and van den Berg, 2014). There was also a direct relationship in this study ($r^2 = 0.95$, $p < 0.05$, $n = 4$) between HS concentrations and the concentration of L_2 ligands (data not shown), suggesting HS may be predominantly part of the L_2 ligand pool. Some of this relationship is likely driven by a similar relationship between HS and [dFe], though a similarly robust relationship does not hold for the concentration of other ligand classes vs. [HS] (data not shown).

The amount of potential dFe binding capacity by HS can be calculated according to the binding capacity of HS measured by Laglera and van den Berg (2009). They reported that HS could bind 32 nmol Fe per mg of HS on average, which results in a range of binding capacities for dFe in San Francisco Bay samples (Fig. 4). Based on this calculation, the concentration of dFe binding that could be accounted for by HS ranges from 0.72 nmol L^{-1} at station 25 in the BBL to 17.9 nmol L^{-1} at station 2 in San Francisco Bay (Fig. 4). The percentage of dFe complexation by HS, in the absence of competition from any other ligands, decreased from 23% at station 2 to 3% at station 26, though there was still a significant percentage of the dFe complexed by HS at station 25 because of the much lower dFe concentrations (Table 1).

The presence of HS was additionally inferred from ^{1}H-NMR in four samples where HS was also determined by CSV (stations 13, 24, 25, and 26) as described in Section 3.6 below.

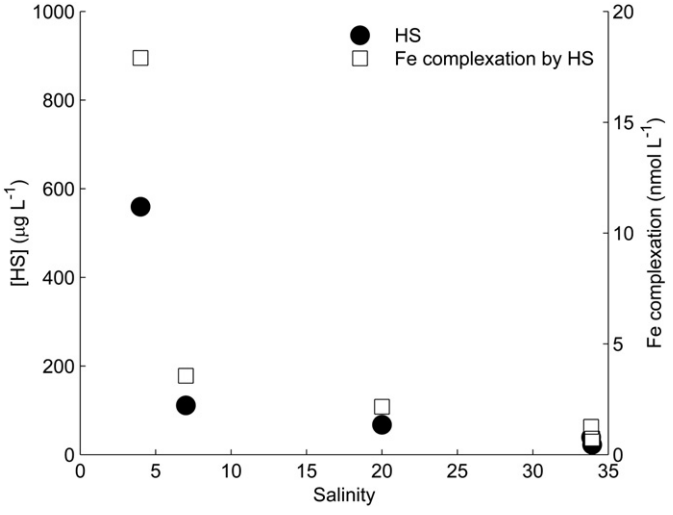

Fig. 4. Humic-like substances (HS) as measured by CSV in San Francisco Bay and in BBL samples plotted versus salinity. The dissolved iron (Fe) complexation accounted for by HS was based on a binding constant of 32 nmol Fe mg^{-1} HS determined by Laglera and van den Berg (2009).

Table 2
Dissolved organic carbon (DOC) concentrations and ^{1}H-NMR integrated area percentages of the major chemical functional groups from stations 13, 24, 25 and 26.

Sta.	DOC	CH_3-C	CH_3-	$CH_x-C-COO/$	CH_3-	$CH_x-COO/$	CHOH	H−Ar/	% CRAM	% HPS	% CRAM
	μmol L^{-1}		Deoxy sugar	CH_x-C-Ar	C=O	CH_x-Ar		H−C=C			× DOC
13	106	13	20	15	9	29	12	1	58	42	6148
24	83	14	23	11	7	29	13	3	57	43	4765
25	79	14	19	11	7	23	22	4	52	48	4094
26	76	8	20	13	8	30	19	2	53	47	4028

3.6. DOC and ^{1}H-NMR analysis

Four samples were analyzed for both DOC and ^{1}H-NMR measurements as a first step in trying to understand the chemical components of the ligand pool coupled to detailed electrochemical measurements (Table 2). Station 13 showed the highest DOC concentrations compared to the other stations (106 μmol L^{-1}, Table 2), which was followed by the other surface station (Station 24, 83 μmol L^{-1}). The two BBL stations (25 and 26) had a very similar DOC concentration, with 79 and 76 μmol L^{-1}, respectively (Table 2).

All ^{1}H-NMR spectra of the DOM from the four stations (Fig. 5) had several bands in common. They all illustrate an intense methyl band (CH_3-C) centered on 1.2 ppm, which could be derived from either the lipids CH_2 group or the CH_3 group of deoxy-sugars. Based on some recent studies, the assignment of these signals is mostly to deoxy-sugars. For example, Panagiotopoulos et al. (2007) used both correlation spectroscopy (COSY) and heteronuclear single quantum coherence (HSQC) NMR analysis to verify that this band is mostly from methyl group of deoxy-sugars in oceanic water samples isolated by ultrafiltration. Also, Abdulla et al. (2013) also showed that this band in ultrafiltration-isolated DOM has a positive correlation with the changes in carbohydrate signatures and a negative correlation with the terminal methyl groups along a salinity transect. Ultrafiltration was not used in the current study, so there is a possibility that lipid-like components are contributing to the DOM and the peak at 1.2 ppm may have some contribution from lipids. A band around 2.0 ppm is attributed mainly to methyl protons of the acetate functional group ($CH_3C=O$) (Aluwihare et al., 1997; Repeta et al., 2002), and a broad band centered at 3.5 ppm was assigned to protons from carbohydrate compounds (CHOH; Aluwihare et al., 1997). Interestingly, all four stations show an absence of unsaturated and aromatic signatures as indicated by missing the very broad band between 6.0 and 9.0 ppm. To estimate the contribution of the major chemical functional groups, each spectrum was divided into seven defined bands according to Abdulla et al. (2013): (1) CH_3-C (0.25–1.02 ppm), (2) CH_3–deoxy sugar (1.02–1.39 ppm), (3) $CH_x-C-COO/CH_x-C-Ar$ (1.39–1.82 ppm), (4) $CH_3-C=O$ (1.82–2.08 ppm), (5) CH_x-COO/CH_x-Ar (2.08–3.25 ppm), (6) CHOH (3.25–5.80 ppm), and (7) H−Ar/H−C=C (5.8–9.00 ppm). The area percentage of each of these functional groups is presented in Table 2. These seven functional groups are classified into two major chemical components: a) carboxylic rich alicyclic molecules (CRAM), which includes band numbers 1, 3, 5 and 7; and b) heteropolysaccharides (HPS), which consists of band numbers 2, 4 and 6 (Hertkorn et al., 2006; Abdulla et al., 2013). The surface stations in San Francisco Bay (13 and 24) had a significantly higher CRAM percentage compared to the BBL stations (25 and 26, Table 2), and the BBL stations had a higher HPS component compared to the two San Francisco Bay stations (Table 2).

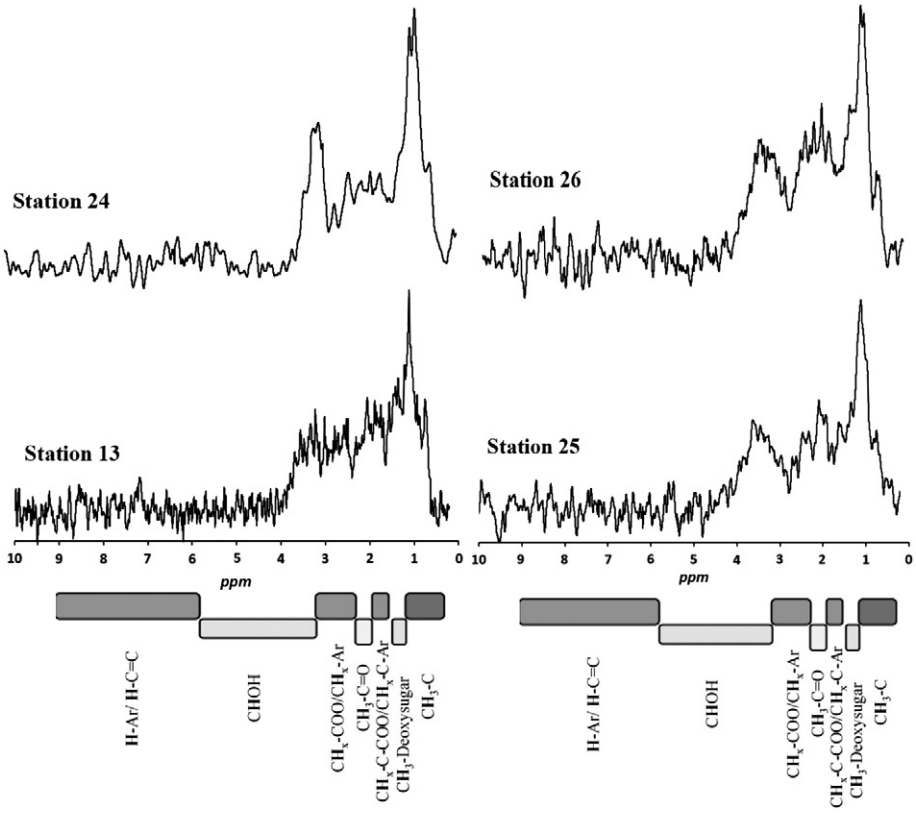

Fig. 5. ^{1}H-NMR spectra of the San Francisco Bay surface water stations (13 and 24, left panels) and the BBL stations (25 and 26, right panels).

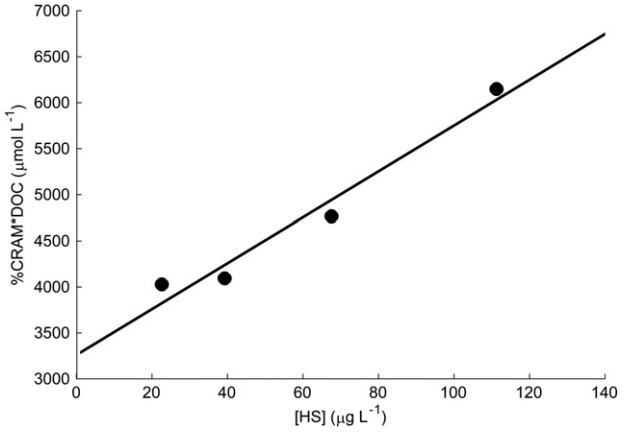

Fig. 6. Relationship between the humic-like substances (HS) concentration as measured by CSV and the magnitude of CRAM in the samples measured by ^{1}H-NMR and DOC concentration ($y = 24.9x + 3260$, $r^2 = 0.96$).

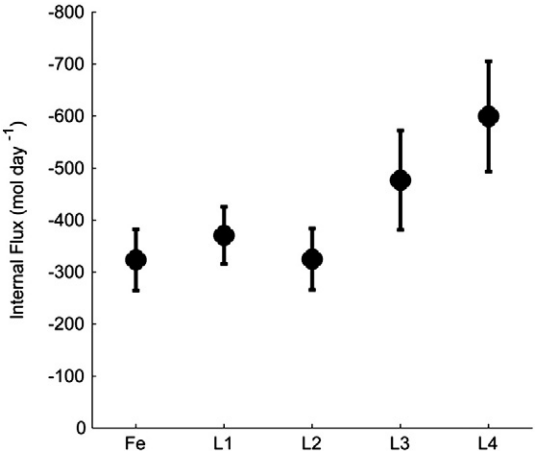

Fig. 7. Internal flux calculations based on Flegal et al. (1991) for dissolved iron (dFe) and dFe-binding ligands (L_1–L_4). Error bars represent the error propagation of the constituent measurement and in the calculation of C_*.

In order to account for the differences in the DOC concentrations between the stations, the area percentage of CRAM of each station was multiplied by its DOC concentration (%CRAM × DOC, Table 2). This normalized CRAM component (%CRAM × DOC) was plotted against [HS] determined by CSV (Fig. 6), and resulted in a strong positive correlation ($r^2 = 0.96$, $p < 0.05$) between the two parameters.

4. Discussion

4.1. The coupling of stronger ligands (L_1 and L_2) and dissolved Fe

The two strongest ligand classes measured in San Francisco Bay have very similar distributions within the estuary (Fig. 3). The excess ligand concentrations (Fig. 3B) reveal that dFe in San Francisco Bay is relatively tightly coupled to the stronger ligand classes, especially in the higher salinity samples where eL_1 and eL_2 approach zero. Buck et al. (2007) was the first to note this close correlation in the San Francisco Bay plume, and suggested the stronger ligands were the most important in stabilizing the [dFe]. This was supported by the fact that leachable particulate Fe concentrations remained high in the plume, while dFe was "capped" at the stronger ligand concentrations (Buck et al., 2007). The same phenomenon was observed in additional samples in the CCS in a follow-up study by Biller et al. (2013) and Bundy et al. (2014), especially within the BBL.

Additional evidence for the tight coupling between dFe and the strongest ligands is apparent when the internal fluxes of each constituent are calculated within the estuary. These fluxes can be estimated according to the methods of Flegal et al. (1991), where the internal flux is defined as $F_{int} = R(C_* - C_0)$, and F_{int} is the flux of the constituent within the estuary (nmol day^{-1}), R is the river discharge (L day^{-1}), C_* is the hypothetical riverine endmember given conservative mixing (nmol L^{-1}), and C_0 is the actual riverine endmember measured at station 2 (nmol L^{-1}). The river discharge (R) was estimated based on a 19 day average of the Sacramento River on the days immediately preceding sample collection in April (http://waterdata.usgs.gov/ca/nwis/current/?type=flow&group_key=basin_cd), and was equal to $7.43 \times 10^9 \pm 1.88 \times 10^9$ L day^{-1}. The value of C_* was estimated according to Flegal et al. (1991) by extrapolating the linear best-fit line from the linear portion of the mixing curve at the highest salinities to the zero salinity endmember, if conservative mixing from seawater alone were considered. When the value of C_* is less than the measured riverine endmember at station 2, then the constituent has an internal sink. These calculations all assume steady state conditions in San Francisco Bay, and that the variation in the freshwater endmember is small compared to the inventory of the constituent (Officer, 1979). Very similar dFe concentrations were obtained in this study compared to others (Flegal et al., 1991; Sañudo-Wilhelmy et al., 1996) despite the differences in sampling seasons. Thus, for the purposes of these approximations, steady state conditions are taken as a valid assumption. Based on this calculation, dFe and the strongest ligands have internal sinks in San Francisco Bay of a similar magnitude (Fig. 7). The magnitude of F_{int} for dFe, L_1 and L_2 was calculated to be -323.5 ± 58.9, -370.3 ± 55.0, and -324.6 ± 59.1 nmol day^{-1}, respectively. These fluxes are statistically indistinct (t-test, $p > 0.05$), and represent very similar processes effecting both dFe and stronger ligands in San Francisco Bay. This is also apparent from the residual analysis in Fig. 8, where residuals are shown as deviations from the best-fit polynomial line through each of the data sets (dFe and ligands). The stronger ligands (L_1 and L_2) and dFe have relatively similar residuals when compared to the weaker ligands, confirming the trends observed in stronger ligands are correlated with those in dFe.

Although there are high concentrations of stronger ligands in the low salinity end of the estuary (Table 1) they are almost completely titrated with dFe, which is made apparent by the low, and sometimes negative, excess ligand concentrations (Fig. 3B). The excess stronger ligands remain fully titrated at the higher salinities and perhaps even slightly increase in the highest salinity sample (Fig. 3B). This suggests that the strongest ligand complexes are the most resistant to flocculation in the estuary, and that dFe is perhaps even further stabilized at

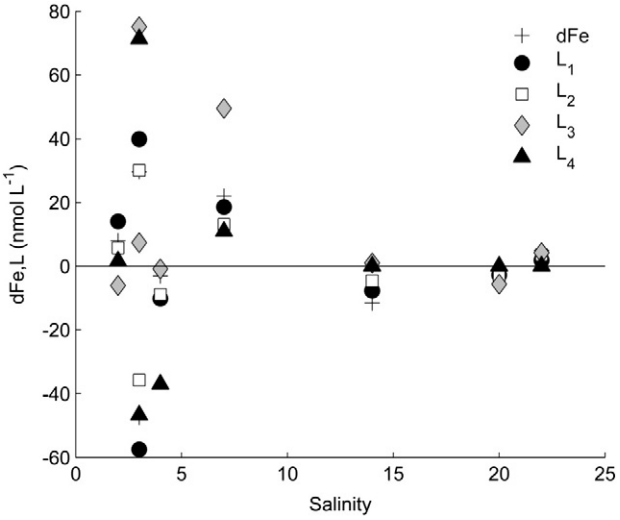

Fig. 8. Residuals from the best-fit second order polynomial line of constituent versus salinity for each individual data set of dissolved iron (dFe), and dFe-binding ligands (L_1, L_2, L_3 and L_4) in San Francisco Bay.

high salinities by a source of stronger ligands from the seawater endmember. Elevated concentrations of strong ligands have been observed in CCS coastal waters (Bundy et al., 2014) so coastal waters may provide a small but significant source of strong ligands to San Francisco Bay and vice versa. In Bundy et al. (2014), two samples were taken from the mouth of San Francisco Bay (on an ebb tide) and those stations contained very high strong ligand concentrations (Bundy et al., 2014; transect 16). Thus, it is not entirely clear whether low salinity waters are the sole source of the stronger ligands observed in San Francisco Bay. Regardless, the stronger ligands appear to prevent some portion of the dFe from precipitating at higher salinities. This was also noted in the Satilla River Estuary, where Jones et al. (2011) observed a strong correlation between dFe–ligand complexes and [dFe] in the estuary, which they hypothesized was accounted for by a portion of the dFe pool bound to strong ligands (Jones et al., 2011).

Krachler et al. (2012) observed a portion of the DOM pool to be completely resistant to flocculation in mixing experiments at high salinities, which they hypothesized to be comprised at least in part by HS (Batchelli et al., 2010). They also found that approximately 16% of the dFe in their study area was bound to small (0.5–3.0 nm) organic molecules which comprised the portion of dFe that was resistant to scavenging (Krachler et al., 2012). These dFe-containing complexes were found to be identical to terrigenous lignin phenols that have been found in many areas of the oceans (Benner et al., 2005; Hernes and Benner, 2002, 2006; Louchouarn et al., 2010; Opsahl and Benner, 1997). Abdulla et al. (2013) showed that the terrestrial CRAM component consists mainly of two different classes of compounds (aliphatic polycarboxyl compounds and lignin-like compounds) and these two classes share similar biogeochemical reactivity along the estuary. Based on this finding, it is expected that the Fe-rich nanoparticles detected by Krachler et al. (2012) are also enriched with aliphatic polycarboxyl compounds as well as lignin-like compounds. In the current study, there was a significant percentage of CRAM in all four samples analyzed by ^{1}H-NMR, suggesting that the CRAM component is relatively consistent across the sampled salinity gradient, although there were only four samples measured. It is likely that the complexation of these compounds with dFe represents at least some portion of the stronger ligand pool seen in this study to be resistant to scavenging.

Many of the siderophores that have been identified in aquatic systems appear to originate from freshwater cyanobacteria (Ito et al., 2004; Simpson and Neilands, 1976; Wilhelm and Trick, 1994) and heterotrophic bacteria (Gledhill et al., 2004; Mawji et al., 2011). Although diatoms clearly dominate in San Francisco Bay (Cloern, 1996; Cloern and Dufford, 2005), cyanobacteria and heterotrophic bacteria are present across large gradients in salinity and appear to be ubiquitous (Cloern and Dufford, 2005). It is, therefore, likely that bacteria may be largely responsible for production of siderophores in San Francisco Bay, which then contribute to the measured strong ligand pool in low salinity waters. The percentage of the CRAM component in the surface samples from San Francisco Bay is slightly higher than the marine BBL samples, and the CRAM component has been linked to dFe binding in other studies (e.g., Abdulla et al., 2010). Isolated siderophores in culture are known to contain carboxylate functional groups (Vraspir and Butler, 2009), but these types of siderophores have not been directly isolated from seawater. Based on the presence of strong ligands and high CRAM components in samples from San Francisco Bay, this study suggests the presence of carboxylate-containing dFe-binding ligands in the estuary, though the extent of their presence is unclear since not all stations were sampled. Although it is not certain how strong the carboxylate-containing organic complexes are with dFe, it is possible that CRAM components may be present in the stronger ligand pools (L_1 and L_2).

4.2. Flocculation of weaker ligands and dissolved iron

The distributions of weaker ligands in San Francisco Bay are distinct from those of the stronger ligand pool (Fig. 3). The L_3 ligands ($\log K^{cond}_{FeL,Fe'} = 10–11$) are high in stations 2–6 (Table 1), but were not detected in mid-salinity samples. They are detected in higher salinity samples again, with slightly elevated [eL_3] over the stronger ligands at these salinities (Fig. 3B). The [eL_3] in the low salinity samples are comparable to [eL_2], though slightly lower than the [eL_4]. The concentrations of L_4 ligands are extremely high in the low salinity end of the North Bay, and are not detectable at salinities higher than 7 (Fig. 3). The fact that L_4 ligands are no longer detectable at higher salinities, and [eL_3] generally declines through the estuary, suggests that most of the dFe lost to flocculation occurs in the portion of dFe bound to weaker ligands.

Internal fluxes of the weaker ligands are also statistically distinct (t-test, $p < 0.005$) from the flux of dFe and stronger ligands in San Francisco Bay (Fig. 7). The internal flux of dFe and strong ligands were all approximately -300 mol day^{-1}, while for L_3 ligands it is -476.6 ± 95.8 mol day^{-1} and -599.2 ± 105.9 for L_4 ligands. This likely reflects the different processes and chemical characteristics of the weaker ligand pool compared to the stronger ligand pool in San Francisco Bay. Although no size-fractioned ligand data is available for this study, it is possible that the majority of the weaker ligand pool is in the colloidal size fraction which has been shown to flocculate more rapidly compared to the soluble fraction (Batchelli et al., 2010; Moore et al, 1979; Murray and Gill, 1978; Sañudo-Wilhelmy et al., 1996; Sholkovitz et al., 1978).

There are a variety of possible sources for weaker ligands in San Francisco Bay, based on evidence from previous studies done on ligands and DOM in this estuary. In the Buck et al. (2007) study of the Columbia River and San Francisco Bay plumes, the authors identified strong ligands in both areas but only detected weaker ligands in the San Francisco Bay plume. This was attributed to the different residence times of the two estuaries, with North San Francisco Bay having a longer residence time (1–60 days; Flegal et al., 1991) than the Columbia River. The authors suggested that weaker ligands might be degradation products of the stronger ligand pool based on the longer flushing time (Buck et al., 2007). Although some weaker ligands were probably undetected in the Columbia River due to the use of a relatively high analytical window ($\alpha_{Fe(SA)_x} = 60$), it is possible that residence time plays a role in the dFe-binding ligand pool. It is also likely that the composition of DOM is important. This is supported by observations of high concentrations of detrital DOM and particulate organic matter (POM) in the low salinity endmember of San Francisco Bay (Murrell and Hollibaugh, 2000) and organic matter fluxes from sediments in Suisun Bay (Murrell and Hollibaugh, 2000). Indeed, higher weaker ligand concentrations are observed in Suisun Bay in this study (stations 4–8) and are likely contributed from sediment resuspension in that area similar to what has been observed in other estuaries with high organic content (Jones et al., 2011). Additional sources of ligands beyond those derived from the San Joaquin and Sacramento Rivers, such as sediment resuspension, are apparent from the residual analysis (Fig. 8), where ligands are elevated at salinities 3–7 in Suisun Bay. It is also possible that adjacent marsh lands are a source of ligands, as elevated copper-binding ligands were also seen in this area in another study (Buck and Bruland, 2005). Besides organic matter from sediments and marsh lands in Suisun Bay, Murrell and Hollibaugh (2000) also found that a large portion of the organic matter in low salinity samples was from remineralization of algal POC, which has been shown in other studies to be a source of weaker ligands and dFe (Boyd et al., 2010).

The ^{1}H-NMR data also provides a first step towards identifying the weaker ligands in San Francisco Bay and in the BBL. The observed flocculation of metals and HS at low salinities in estuaries (Boyle et al., 1977; Sholkovitz et al., 1978) and the loss of weaker ligands at high salinities indicate that some portion of HS is likely also part of the weaker ligand pool, despite its relatively elevated conditional stability constant (Laglera and van den berg, 2009). This is also supported by the decline in dFe complexation by HS at higher salinities (Fig. 4). In addition to HS, Table 2 indicates that a high percentage of heteropolysaccharide

(HPS) components were found in all four samples analyzed. Although polysaccharides were not measured in this study and have not been measured directly in San Francisco Bay, high concentrations of carbohydrates have been observed in estuaries (Abdulla et al., 2013; Wang et al., 2010) and shown to decline non-conservatively with salinity (Wang et al., 2010). Polysaccharides have the potential to transfer carbon from the dissolved to particulate pools (Santschi et al., 2003), which could, in turn, lead to flocculation of polysaccharides and associated trace metals in the estuary. Wang et al. (2010) observed a 5–10% loss of carbohydrates in the Bay of Saint Louis in the northern Gulf of Mexico due to physical mixing alone. Terrestrial polysaccharides contain galacturonic acid, which can bind Fe. It is therefore possible that these terrestrial polysaccharides represent a portion of the dFe-binding ligand pool in San Francisco Bay. Polysaccharides have been observed in coastal waters and in the open ocean in other studies (Abdulla et al., 2013; Aluwihare et al., 1997, 2002; Benner et al., 1992; Repeta et al., 2002), and they have been previously implicated as an important component of the weaker dFe-binding ligand pool (Hassler et al., 2011a), but this has not been tested directly in estuaries. DFe bound to polysaccharides has been found to have enhanced reactivity and bioavailability to eukaryotic phytoplankton in the Southern Ocean (Hassler et al., 2011b), and thus may render the dFe bound to weaker ligands in the BBL and San Francisco Bay relatively bioavailable to coastal and estuarine phytoplankton.

4.3. Contribution of humic-like substances to the iron-binding ligand pool

Humic-like substances (HS) were found to be an important component of the dFe-binding ligand pool in this study, potentially complexing 23% of the dFe in San Francisco Bay. HS, like dFe and ligands, appear to behave non-conservatively within the estuary (Fig. 4). This observation supports the finding that HS likely contribute to the pool of dFe-binding ligands that are flocculated in the estuary (Boyle et al., 1977; Sholkovitz et al., 1978). However, there is also some evidence that HS are not only components of the weaker ligand pool that are scavenged, but part of the stronger ligand classes less prone to flocculation as well. HS measurements made by CSV in our study (Table 1) and previous work (Abualhaija and van den Berg, 2014; Bundy et al., 2014; Laglera and van den Berg, 2009) have found that HS is likely part of the L_2 ligand pool since the log $K^{cond}_{FeL,Fe'}$ for HS (11.1–11.6) falls in the L2 range (log K = 11–12), although there may be an even larger range of binding strengths for HS. The estimation of the CRAM component by ^{1}H-NMR provides supporting evidence for the presence of HS in these samples, where CRAM components show a positive correlation with [HS] measured by the CSV method (Fig. 6). However, the positive y-intercept in Fig. 6 may indicate either that the CSV method underestimates the concentration of aliphatic carboxyl ligand (in HS) or that there are wide variations in the degree of carboxylation among the compounds within the CRAM component, and only the compounds with a high degree of carboxylation (polycarboxyl compounds) will act as strong ligands for Fe while the compounds with a lower degree of carboxylation (e.g. one or two carboxyl functional group per compound) will act as weaker ligands. This is an important aspect of HS and dFe interactions that requires further investigation, and might explain the apparent presence of HS in several ligand classes.

The strong correlation between CRAM and HS measured by CSV here, as well as data from other studies (e.g., Abdulla et al., 2010), supports the concept that aliphatic polycarboxyl compounds act as strong ligands for dFe. From a theoretical point of view according to the hard and soft acids and bases (HSAB) concept (Pearson, 1963), the high negative charge density of the carboxyl group makes it an ideal strong Lewis base group to bind with strong Lewis acids like Fe^{3+} (Bertini, 2007; Kaim and Schwederski, 1994). Many studies have shown that carboxyl groups of HS are major binding sites of complexed dFe (Byler et al., 1987; Karlsson and Persson, 2010; Kung and Mcbride, 1989; Schnitzer and Skinner, 1963). In addition, based on Fourier transform infrared spectroscopy (FTIR) analysis, Abdulla et al. (2010) found that ~60% of the carboxyl groups in high molecular weight (HMW) DOM isolated from the Great Dismal Swamp (Virginia) appeared to be bound to dFe. Based on this evidence, it appears that HS varies widely in terms of its ability to complex dFe, likely related to its size fraction and the degree of carboxylation of HS compounds.

The potential partitioning of HS into several dFe-binding ligand groups is not surprising, given previous observations from other coastal environments. Batchelli et al. (2010) saw HS in both the soluble and colloidal fractions in Thurso Bay, with the colloidal fraction behaving non-conservatively and the soluble fraction mixing conservatively. Previous studies suggested that the soluble strong ligand pool observed may be comprised of siderophores that can effectively compete for dFe bound to HS because of reversible binding to HS (Batchelli et al., 2010; Laglera et al., 2007). HS measured by CSV can also capture a wide range of complexes, including humic and fulvic acids (Laglera et al., 2007). The HS may also not be only terrestrially-derived; Guo et al. (2000) noted that a significant portion of the colloidal HS material found outside of Galveston Bay may have derived from phytoplankton, based on the metal to organic carbon ratios (Guo et al., 2000). Several studies on organic matter cycling in estuaries have noted a gradient in the size distribution of organic matter complexes through an estuary, ranging from high molecular weight complexes at the low salinity end to low molecular weight complexes at the marine endmember (Moore et al., 1979; Murray and Gill, 1978; Murrell and Hollibaugh, 2000; Sholkovitz et al., 1978), supporting the transition from weaker to strong ligands observed in this study and the potential presence of HS in more than one ligand class in San Francisco Bay. Collectively, these observations suggest that the HS pool in estuaries is heterogeneous and dynamic, and likely plays an important role in the cycling and transport of dFe in San Francisco Bay and surrounding coastal waters.

4.4. Freshwater influences on coastal California Current waters

San Francisco Bay appears to influence California Current shelf waters as a source of both dFe and strong dFe-binding ligands. Although almost 90% of the dFe from the Sacramento and San Joaquin rivers is lost in the estuary before reaching the shelf, the remaining dFe is strongly bound by organic ligands resistant to flocculation. The scavenged Fe is likely deposited on the shelf or in the estuary and transported to the shelf, associated with weaker ligands and HS, and may be further processed in the surface sediments. The presence of HS both in the estuary and on the shelf outside of San Francisco Bay and Eel River (Table 1), and the similarity in CRAM components between low salinity samples to BBL samples (Fig. 5), also suggest that some of the BBL ligand pool is comprised of HS derived from estuarine sources. It is therefore likely that this pool of dFe and ligands is responsible for the pulse of upwelled dFe from the shelf in early spring upwelling events in the coastal CCS, as the "capacitor" hypothesis suggests. Due to reversible binding of dFe by strong dFe-binding ligands in surface waters in the CCS (Bundy et al., 2014), much of this upwelled dFe is likely available to phytoplankton and helps to fuel primary productivity along the California coast.

Acknowledgements

We thank the Captain and crew of the R/V Polaris for their sampling support. We would also like to thank Tara Schraga, Jessica Dyke, and Valerie Greene and the rest of the USGS San Francisco Bay water monitoring team for logistical support. R.M.B. and K.A.B. were supported by NSF grant OCE 10-26607 for the California Current Ecosystem Long Term Ecological Research (LTER) program. H.A. and P.G.H. were supported by Batten Endowment, D.B was supported by NSF grant OCE 0849943 to Ken Bruland, and K.N.B. and San Francisco bay sampling activities were supported by CALFED Bay-Delta Science Fellowship

U-04-SC-005 for Sea Grant Project #R/SF-32. We thank two anonymous reviewers and Maeve Lohan for their helpful comments and insights.

Appendix A. Supplementary data

Supplementary data to this article can be found online at http://dx.doi.org/10.1016/j.marchem.2014.11.005.

References

Abdulla, H.A.N., Minor, E.C., Dias, R.F., Hatcher, P.G., 2010. Changes in the compound classes of dissolved organic matter along an estuarine transect: a study using FTIR and C-13 NMR. Geochim. Cosmochim. Acta 74 (13).

Abdulla, H.A.N., Minor, E.C., Dias, R.F., Hatcher, P.G., 2013. Transformations of the chemical compositions of high molecular weight DOM along a salinity transect: using two dimensional correlation spectroscopy and principal component analysis approaches. Geochim. Cosmochim. Acta 118, 231–246.

Abualhaija, M.M., van den Berg, C.M., 2014. Chemical speciation of iron in seawater using catalytic cathodic stripping voltammetry with ligand competition against salicylaldoxime. Mar. Chem. 164, 60–74.

Aluwihare, L.I., Repeta, D.J., Chen, R.F., 1997. A major biopolymeric component to dissolved organic carbon in surface sea water. Nature 387 (6629), 166–169.

Aluwihare, L.I., Repeta, D.J., Chen, R.F., 2002. Chemical composition and cycling of dissolved organic matter in the Mid-Atlantic Bight. Deep-Sea Res. I 49 (20), 4421–4437.

Batchelli, S., Muller, F.L.L., Chang, K.-C., Lee, C.-L., 2010. Evidence for strong but dynamic iron–humic colloidal associations in humic-rich coastal waters. Environ. Sci. Technol. 44 (22), 8485–8490.

Benner, R., Pakulski, J.D., McCarthy, M., Hedges, J.I., Hatcher, P.G., 1992. Bulk chemical characteristics of dissolved organic-matter in the ocean. Science 255 (5051), 1561–1564.

Benner, R., Louchouarn, P., Amon, R.M.W., 2005. Terrigenous dissolved organic matter in the Arctic Ocean and its transport to surface and deep waters of the North Atlantic. Glob. Biogeochem. Cycles 19 (2).

Bertini, I., 2007. Biological Inorganic Chemistry: Structure and Reactivity. University Science Books.

Biller, D.V., Bruland, K.W., 2012. Analysis of Mn, Fe, Co, Ni, Cu, Zn, Cd, and Pb in seawater using the Nobias-chelate PA1 resin and magnetic sector inductively coupled plasma mass spectrometry (ICP-MS). Mar. Chem. 130, 50–70.

Biller, D.V., Bruland, K.W., 2014. The central California Current transition zone: a broad region exhibiting evidence for iron limitation. Prog. Oceanogr. 120, 370–382.

Biller, D.V., Coale, T.H., Till, R.C., Smith, G.J., Bruland, K.W., 2013. Coastal iron and nitrate distributions during the spring and summer upwelling season in the central California Current upwelling regime. Cont. Shelf Res. 66, 58–72.

Boyd, P.W., Ibisanmi, E., Sander, S.G., Hunter, K.A., Jackson, G.A., 2010. Remineralization of upper ocean particles: implications for iron biogeochemistry. Limnol. Oceanogr. 55 (3), 1271–1288.

Boyle, E.A., Edmond, J.M., Sholkovitz, E.R., 1977. Mechanism of iron removal in estuaries. Geochim. Cosmochim. Acta 41 (9), 1313–1324.

Bruland, K.W., Rue, E.L., Smith, G.J., 2001. Iron and macronutrients in California coastal upwelling regimes: implications for diatom blooms. Limnol. Oceanogr. 46 (7).

Bruland, K.W., Rue, E.L., Smith, G.J., DiTullio, G.R., 2005. Iron, macronutrients and diatom blooms in the Peru upwelling regime: brown and blue waters of Peru. Mar. Chem. 93 (2–4), 81–103.

Buck, K.N., Bruland, K.W., 2005. Copper speciation in San Francisco Bay: a novel approach using multiple analytical windows. Mar. Chem. 96 (1–2), 185–198.

Buck, K.N., Lohan, M.C., Berger, C.J.M., Bruland, K.W., 2007. Dissolved iron speciation in two distinct river plumes and an estuary: implications for riverine iron supply. Limnol. Oceanogr. 52 (2), 843–855.

Buck, K.N., et al., 2012. The organic complexation of iron and copper: an intercomparison of competitive ligand exchange–adsorptive cathodic stripping voltammetry (CLE–ACSV) techniques. Limnol. Oceanogr. Methods 10, 496–515.

Bundy, R.M., Biller, D.V., Buck, K.N., Bruland, K.W., Barbeau, K.A., 2014. Distinct pools of dissolved iron-binding ligands in the surface and benthic boundary layer of the California Current. Limnology and Oceanography 59(3). Elsevier, pp. 769–787.

Byler, D.M., Gerasimowicz, W.V., Susi, H., Schnitzer, M., 1987. FT-IR spectra of soil constituents — fulvic-acid and fulvic-acid complex with ferric ions. Appl. Spectrosc. 41 (8), 1428–1430.

Cabaniss, S.E., 1991. Carboxylic-acid content of a fulvic-acid determined by potentiometry and aqueous Fourier-transform infrared spectrometry. Anal. Chim. Acta. 255 (1), 23–30.

Chase, Z., Strutton, P.G., Hales, B., 2007. Iron links river runoff and shelf width to phytoplankton biomass along the U.S. West Coast. Geophys. Res. Lett. 34 (4).

Cloern, J.E., 1996. Phytoplankton bloom dynamics in coastal ecosystems: a review with some general lessons from sustained investigation of San Francisco Bay, California. Rev. Geophys. 34 (2).

Cloern, J.E., Dufford, R., 2005. Phytoplankton community ecology: principles applied in San Francisco Bay. Mar. Ecol. Prog. Ser. 285, 11–28.

Elrod, V.A., Berelson, W.M., Coale, K.H., Johnson, K.S., 2004. The flux of iron from continental shelf sediments: a missing source for global budgets. Geophys. Res. Lett. 31 (12).

Elrod, V.A., Johnson, K.S., Fitzwater, S.E., Plant, J.N., 2008. A long-term, high-resolution record of surface water iron concentrations in the upwelling-driven central California region. J. Geophys. Res. C Oceans 113, 21–34.

Flegal, A.R., Smith, G.J., Gill, G.A., Sañudo-Wilhelmy, S., Anderson, L.C.D., 1991. Dissolved trace-element cycles in the San-Francisco Bay estuary. Mar. Chem. 36 (1–4).

Giambalvo, E., 1997. A new method for modeling coupled equilibrium and non-equilibrium chemical reactions. (M.S. thesis) University of California, Santa Cruz.

Gledhill, M., Buck, K.N., 2012. The organic complexation of iron in the marine environment: a review. Front. Microbiol. 3, 69.

Gledhill, M., van Den Berg, C.M.G., 1994. Determination of complexation of iron(III) with natural organic complexing ligands in seawater using cathodic stripping voltammetry. Mar. Chem. 47 (1), 41–54.

Gledhill, M., et al., 2004. Production of siderophore type chelates by mixed bacterioplankton populations in nutrient enriched seawater incubations. Mar. Chem. 88 (1–2), 75–83.

Guo, L.D., Santschi, P.H., Warnken, K.W., 2000. Trace metal composition of colloidal organic material in marine environments. Mar. Chem. 70 (4), 257–275.

Hassler, C.S., Alasonati, E., Nichols, C.A.M., Slaveykova, V.I., 2011a. Exopolysaccharides produced by bacteria isolated from the pelagic Southern Ocean - Role in Fe binding, chemical reactivity, and bioavailability. Mar. Chem. 123 (1–4), 88–98.

Hassler, C.S., Schoemann, V., Nichols, C.M., Butler, E.C.V., Boyd, P.W., 2011b. Saccharides enhance iron bioavailability to Southern Ocean phytoplankton. Proc. Natl. Acad. Sci. U. S. A. 108 (3), 1076–1081.

Hatcher, P.G., Breger, I.A., Earl, W.L., 1981. Nuclear magnetic resonance studies of ancient buried wood—I. Observations on the origin of coal to the brown coal stage. Org. Geochem. 3 (1), 49–55.

Hernes, P.J., Benner, R., 2002. Transport and diagenesis of dissolved and particulate terrigenous organic matter in the North Pacific Ocean. Deep-Sea Res. I 49 (12), 2119–2132.

Hernes, P.J., Benner, R., 2006. Terrigenous organic matter sources and reactivity in the North Atlantic Ocean and a comparison to the Arctic and Pacific oceans. Mar. Chem. 100 (1–2), 66–79.

Hertkorn, N., Benner, R., Frommberger, M., Schmitt-Kopplin, P., Witt, M., Kaiser, K., Kettrup, A., Hedges, J.I., 2006. Characterization of a major refractory component of marine dissolved organic matter. Geochim. Cosmochim. Acta 70 (12), 2990–3010.

Hudson, R.J.M., Rue, E.L., Bruland, K.W., 2003. Modeling complexometric titrations of natural water samples. Environ. Sci. Technol. 37 (8), 1553–1562.

Hutchins, D.A., DiTullio, G.R., Zhang, Y., Bruland, K.W., 1998. An iron limitation mosaic in the California upwelling regime. Limnol. Oceanogr. 43 (6), 1037–1054.

Ito, Y., Ishida, K., Okada, S., Murakami, M., 2004. The absolute stereochemistry of anachelins, siderophores from the cyanobacterium Anabaena cylindrica. Tetrahedron 60 (41), 9075–9080.

Johnson, K.S., et al., 2007. Developing standards for dissolved iron in seawater. EOS Trans. AGU 88 (11), 131–132.

Jones, M.E., Beckler, J.S., Taillefert, M., 2011. The flux of soluble organic–iron(III) complexes from sediments represents a source of stable iron(III) to estuarine waters and to the continental shelf. Limnol. Oceanogr. 56 (5), 1811–1823.

Kaim, W., Schwederski, B., 1994. Bioinorganic Chemistry: Inorganic Chemistry in the Chemistry of Life. Wiley, Chichester, UK.

Karlsson, T., Persson, P., 2010. Coordination chemistry and hydrolysis of Fe(III) in a peat humic acid studied by X-ray absorption spectroscopy. Geochim. Cosmochim. Acta 74 (1), 30–40.

King, A.L., Barbeau, K., 2007. Evidence for phytoplankton iron limitation in the southern California Current System. Mar. Ecol. Prog. Ser. 342, 91–103.

Kogut, M.B., Voelker, B.M., 2001. Strong copper-binding behavior of terrestrial humic substances in seawater. Environ. Sci. Technol. 35 (6), 1149–1156.

Krachler, R., et al., 2012. Nanoscale lignin particles as sources of dissolved iron to the ocean. Glob. Biogeochem. Cycles 26.

Kung, K.H., McBride, M.B., 1989. Adsorption of para-substituted benzoates on iron-oxides. Soil Sci. Soc. Am. J. 53 (6), 1673–1678.

Laglera, L.M., van den Berg, C.M.G., 2009. Evidence for geochemical control of iron by humic substances in seawater. Limnol. Oceanogr. 54 (2), 610–619.

Laglera, L.M., Battaglia, G., van den Berg, C.M.G., 2007. Determination of humic substances in natural waters by cathodic stripping voltammetry of their complexes with iron. Anal. Chim. Acta. 599, 58–66.

Laglera, L.M., Battaglia, G., van den Berg, C.M.G., 2011. Effect of humic substances on the iron speciation in natural waters by CLE/CSV. Mar. Chem. 127 (1–4), 134–143.

Lam, B., Simpson, A.J., 2008. Direct ^{1}H NMR spectroscopy of dissolved organic matter in natural waters. Analyst 133 (2), 263–269.

Leenheer, J.A., Barber, L.B., Amy, G.L., Chapra, S.C., 1995. Sewage contamination in the upper Mississippi River as measured by the fecal sterol, coprostanol. Water Res. 29 (6), 1427–1436.

Liu, X.W., Millero, F.J., 2002. The solubility of iron in seawater. Mar. Chem. 77 (1), 43–54.

Louchouarn, P., et al., 2010. Analysis of lignin-derived phenols in standard reference materials and ocean dissolved organic matter by gas chromatography/tandem mass spectrometry. Mar. Chem. 118 (1–2), 85–97.

Mantoura, R.F.C., Riley, J.P., 1975. Analytical concentration of humic substances from natural-waters. Anal. Chim. Acta. 76 (1), 97–106.

Mawji, E., et al., 2011. Production of siderophore type chelates in Atlantic Ocean waters enriched with different carbon and nitrogen sources. Mar. Chem. 124 (1–4), 90–99.

Moore, R.M., Burton, J.D., Williams, P.J.L., Young, M.L., 1979. Behavior of dissolved organic material, iron and manganese in estuarine mixing. Geochim. Cosmochim. Acta 43 (6), 919–926.

Murray, J.W., Gill, G., 1978. Geochemistry of iron in Puget Sound. Geochim. Cosmochim. Acta 42 (1), 9–19.

Murrell, M.C., Hollibaugh, J.T., 2000. Distribution and composition of dissolved and particulate organic carbon in northern San Francisco Bay during low flow conditions. Estuar. Coast. Shelf Sci. 51 (1), 75–90.

Officer, C.B., 1979. Discussion of the behavior of nonconservative dissolved constituents in estuaries. Estuar. Coast. Mar. Sci. 9, 91–94.

Omanović, D., Garnier, C., Pižeta, I., 2015. ProMCC: an all-in-one tool for trace metal complexation studies. Mar. Chem 173, 25–39.
Opsahl, S., Benner, R., 1997. Distribution and cycling of terrigenous dissolved organic matter in the ocean. Nature 386 (6624), 480–482.
Panagiotopoulos, C., Repeta, D.J., Johnson, C.G., 2007. Characterization of methyl sugars, 3-deoxysugars and methyl deoxysugars in marine high molecular weight dissolved organic matter. Org. Geochem. 38 (6), 884–896.
Pearson, Ralph G., 1963. Hard and soft acids and bases. J. Am. Chem. Soc. 85 (22), 3533–3539.
Pižeta, I., et al., 2014w. Intercalibration exercise with simulated titration data as a first step to best practice guide. Marine ChemistryElsevier (in review).
Poorvin, L., et al., 2011. A comparison of Fe bioavailability and binding of a catecholate siderophore with virus-mediated lysates from the marine bacterium Vibrio alginolyticus PWH3a. J. Exp. Mar. Biol. Ecol. 399 (1), 43–47.
Repeta, D.J., Quan, T.M., Aluwihare, L.I., Accardi, A.M., 2002. Chemical characterization of high molecular weight dissolved organic matter in fresh and marine waters. Geochim. Cosmochim. Acta 66 (6), 955–962.
Rue, E.L., Bruland, K.W., 1995. Complexation of iron(III) by natural organic-ligands in the central North Pacific as determined by a new competitive ligand equilibration adsorptive cathodic stripping voltammetric method. Mar. Chem. 50 (1–4), 117–138.
Sander, S.G., Hunter, K.A., Harms, H., Wells, M., 2011. Numerical approach to speciation and estimation of parameters used in modeling trace metal bioavailability. Environ. Sci. Technol. 45 (15), 6388–6395.
Santschi, P.H., et al., 2003. Control of acid polysaccharide production and Th-234 and POC export fluxes by marine organisms. Geophys. Res. Lett. 30 (2).
Sañudo-Wilhelmy, S.A., RiveraDuarte, I., Flegal, A.R., 1996. Distribution of colloidal trace metals in the San Francisco Bay estuary. Geochim. Cosmochim. Acta 60 (24), 4933–4944.
Scatchard, G., 1949. The attractions of proteins for small molecules and ions. Ann. N. Y. Acad. Sci. 51 (4), 660–672.
Schnitzer, M., Skinner, S.I.M., 1963. Organo-metallic interactions in soils: 1. Reactions between a number of metal ions and the organic matter of a podzol Bh horizon. Soil Sci. 96 (2), 86–93.
Sholkovitz, E.R., Boyle, E.A., Price, N.B., 1978. Removal of dissolved humic acids and iron during estuarine mixing. Earth Planet. Sci. Lett. 40 (1), 130–136.
Simpson, F.B., Neilands, J.B., 1976. Siderochromes in cyanophyceae — isolation and characterization of schizokinen from Anabeana-Sp. J. Phycol. 12 (1), 44–48.
Sohrin, Y., et al., 2008. Multielemental determination of GEOTRACES key trace metals in seawater by ICPMS after preconcentration using an ethylenediaminetriacetic acid chelating resin. Anal. Chem. 80 (16), 6267–6273.
Stevenson, F.J., 1994. Humus Chemistry: Genesis, Composition, Reactions. John Wiley & Sons.
van den Berg, C.M.G., 1995. Evidence for organic complexation of iron in seawater. Mar. Chem. 50 (1–4), 139–157.
Velasquez, I., et al., 2011. Detection of hydroxamate siderophores in coastal and Sub-Antarctic waters off the South Eastern Coast of New Zealand. Mar. Chem. 126 (1–4), 97–107.
Vraspir, J.M., Butler, A., 2009. Chemistry of marine ligands and siderophores. Annu. Rev. Mar. Sci. 1, 43–63.
Wang, X., Cai, Y., Guo, L., 2010. Preferential removal of dissolved carbohydrates during estuarine mixing in the Bay of Saint Louis in the northern Gulf of Mexico. Mar. Chem. 119 (1), 130–138.
Wilhelm, S.W., Trick, C.G., 1994. Iron-limited growth of cyanobacteria — multiple siderophore production is a common response. Limnol. Oceanogr. 39 (8), 1979–1984.